

Source characterization of carbon monoxide and ozone over the Northwestern Pacific in summer 2012

Keyhong Park¹, and Tae Siek Rhee¹

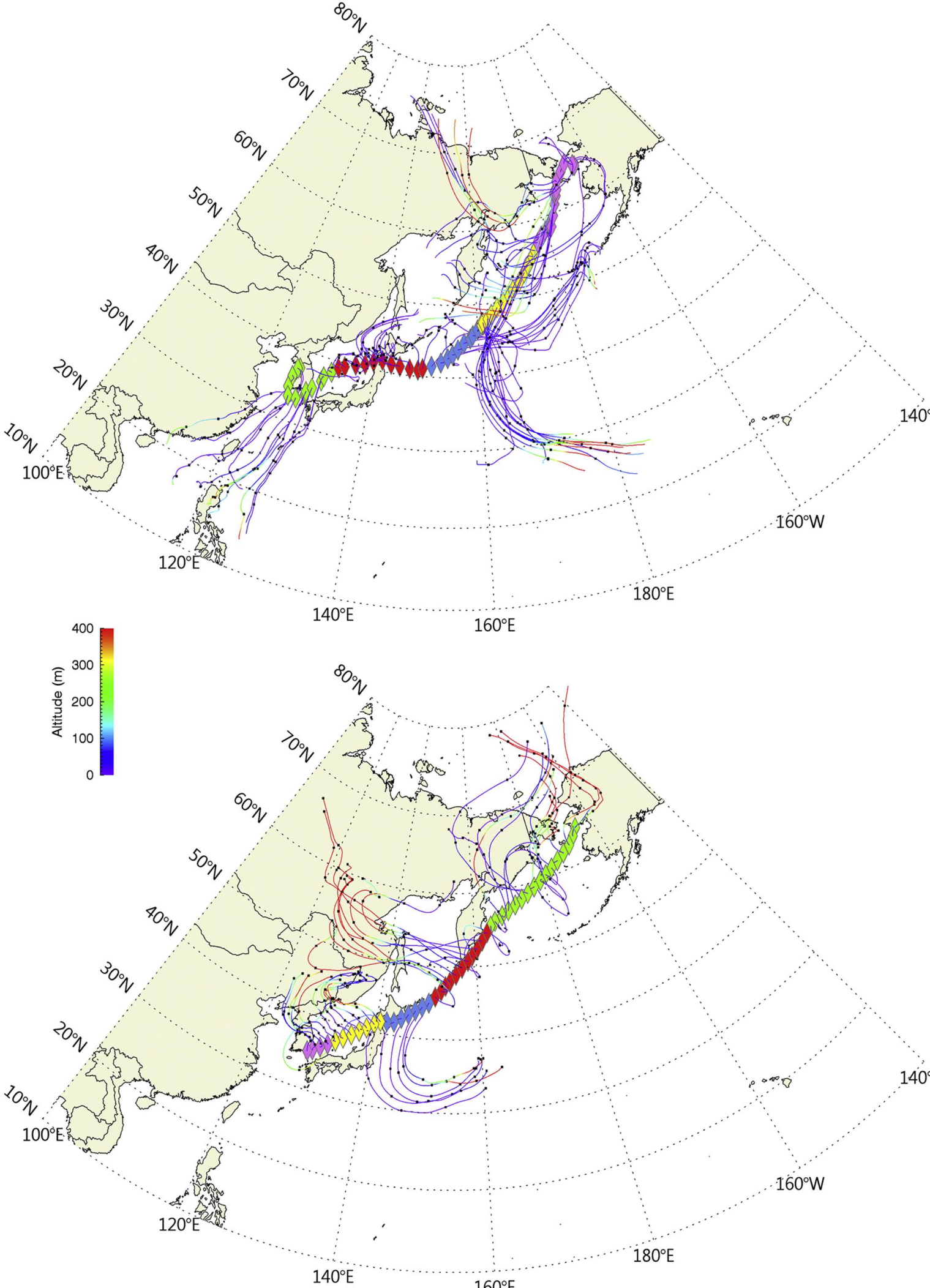
¹ Korea Polar Research Institute, Incheon, South Korea



Abstract

Carbon monoxide (CO) and ozone (O₃) were continuously measured in the marine boundary layer of the East Sea, the Northwestern Pacific, and the Bering Sea onboard R/V Araon in the second halves of July and September of 2012, as a part of the SHIPPO program. Depending on the characteristics of each section of the cruise track, up to 66 ppbv and 17 ppbv of CO and O₃ variability were observed, respectively. The O₃/CO ratio suggests that O₃ was dominantly produced by photochemical reactions in the troposphere, although in the northern sections of the cruise track, the ratio likely suggests vertical transport from the free troposphere or the lowermost stratosphere. To analyze the source characteristics and the transport of both trace gases, a tagging technique in a 3-D global chemical transport model (Model for OZone And Related chemical Tracers-4; MOZART-4) was applied. The model reproduced the observations fairly well, and the technique enabled us to characterize the source regions and composition of the observed CO. Anthropogenic emissions from Northeastern Asian countries appeared to be substantial sources of the CO in the southern sections, and biomass burning in Siberia was an important source of the CO observed in the northern sections of the cruise track. Long-range transport of anthropogenic CO emissions was distinct over the Bering Sea, where the comparable contributions from North America, Northeast Asia, and Europe were identified. Low CO events driven by southern hemispheric invasion were encountered at the southern coast of the Korean peninsula and in the North Pacific at ~50N latitude. The model pointed to a noticeable contribution from the open ocean in the Southern Hemisphere for these events.

SHIPPO 2012 Cruise Track

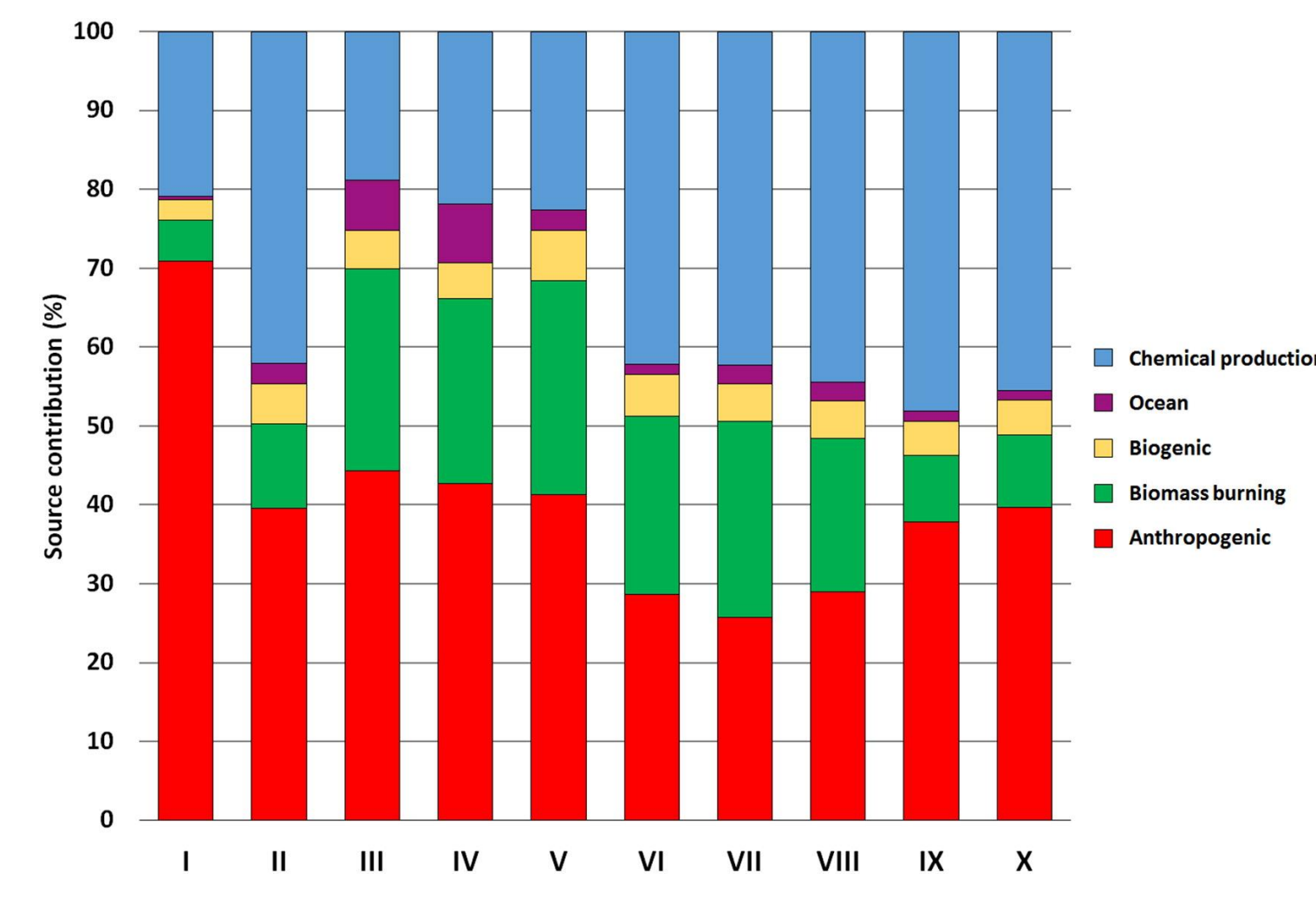
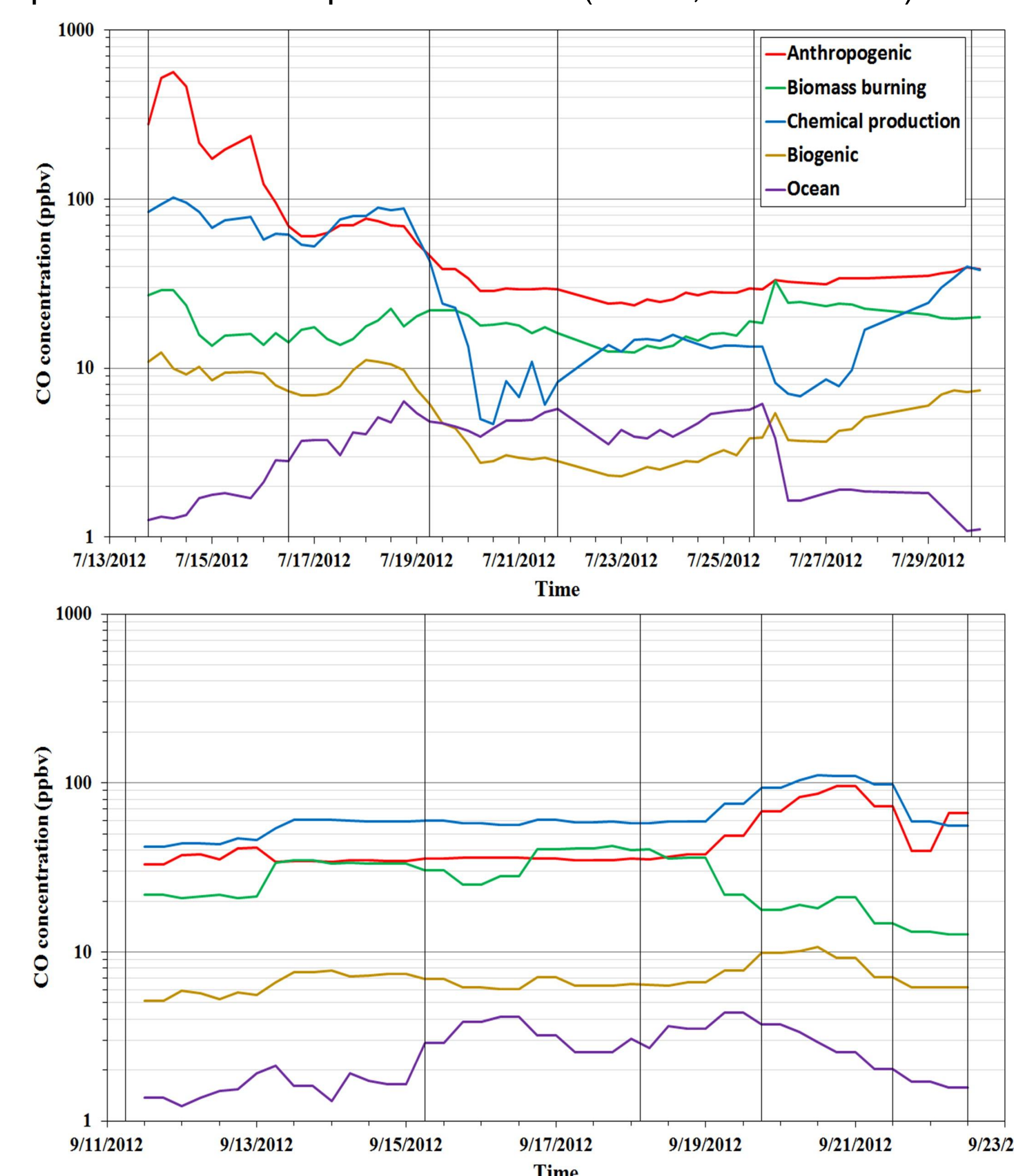


HYSPLIT 5-day backward trajectories calculated every 6 h along the cruise track. The top panel shows the July cruise from Incheon, Korea, to Nome Alaska, U.S.A., and the bottom panel shows the September cruise from Nome Alaska, U.S.A., to Busan, Korea. The color codes indicate the sections of the cruise track defined in the table. Green, red, blue, yellow, and violet correspond to sections I to IV in the top panel, and the same order of colors corresponds to sections VI to X in the bottom panel. (For interpretation of the references to colour in this figure legend, the reader is referred to the web version of this article.)

Name	ID	Start	End
South Asia	I	7/13/2012 18h	7/16/2012 12h
Northern Japan	II	7/16/2012 12h	7/19/2012 06h
Aleutian Islands	III	7/19/2012 06h	7/21/2012 18h
North Pacific	IV	7/21/2012 18h	7/25/2012 14h
Siberia	V	7/25/2012 14h	7/29/2012 20h
Arctic Sea/East Siberia	VI	9/11/2012 18h	9/15/2012 18h
Siberia/Okhotsk Sea	VII	9/15/2012 18h	9/18/2012 15h
North Pacific	VIII	9/18/2012 15h	9/20/2012 06h
Northern East Sea	IX	9/20/2012 06h	9/22/2012 00h
Korean Peninsula	X	9/22/2012 00h	9/23/2012 00h

CO source composition

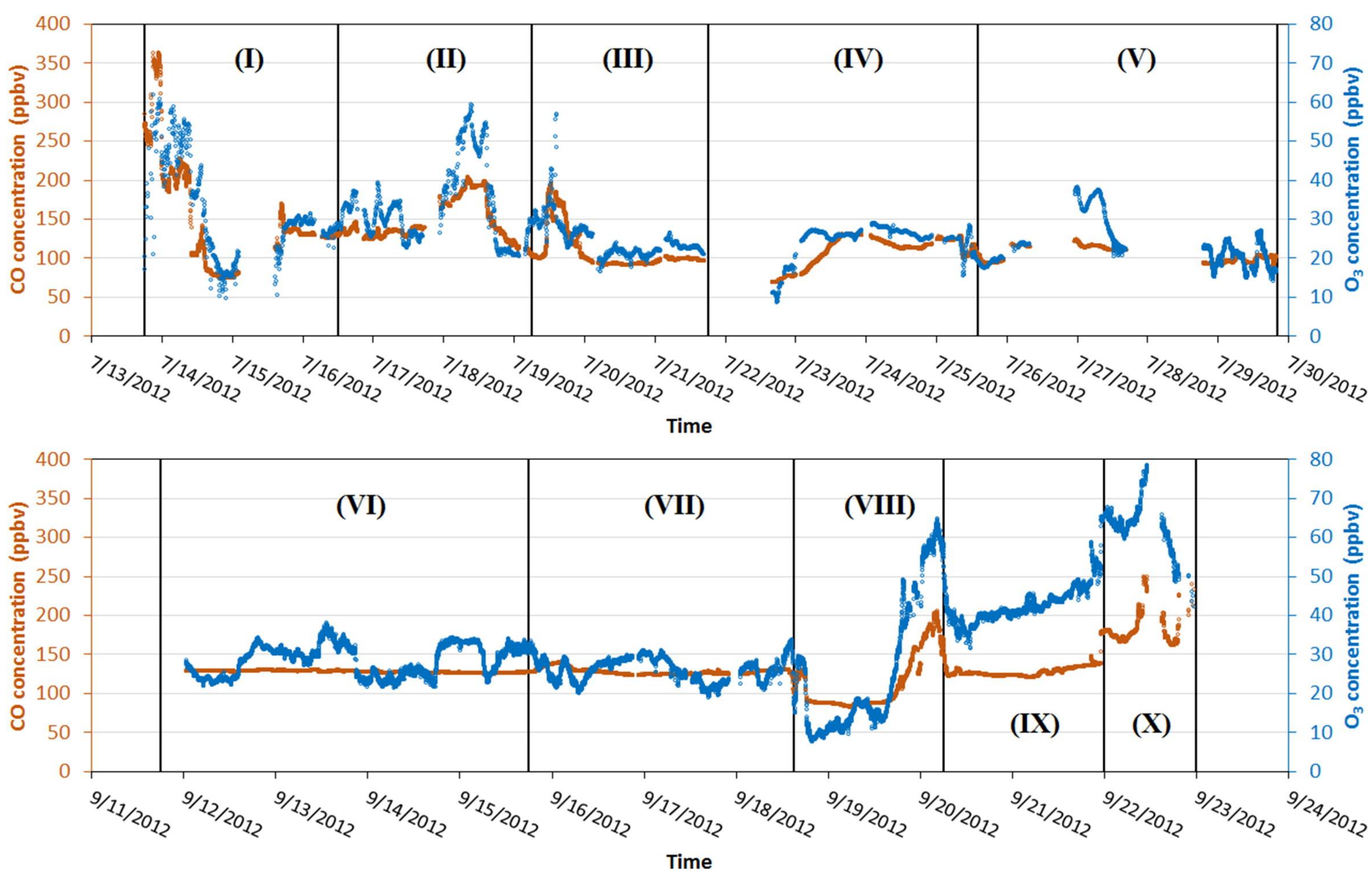
Variation of the CO source composition that was calculated from the tagged MOZART-4 simulation. The upper panel is for the July cruise (Incheon – Nome, AK), and the bottom panel is for the September cruise (Nome, AK – Busan).



Relative source strengths of CO in each section

Chemical production composes all of the CO produced by photochemical reactions in the troposphere. This is the biggest source of CO in the troposphere. In September, we found it predominant among the sources as its contribution was 65 ppbv on average. In July, when the photochemical destruction (CO + OH) was strong, its net contribution decreased and was quite different to anthropogenic emissions. The influence of anthropogenic emissions prevailed over Northeast Asia in both the July (sections I and II) and September cruises (sections IX and X). In particular, the CO in section I was predominantly composed of the anthropogenic sources.

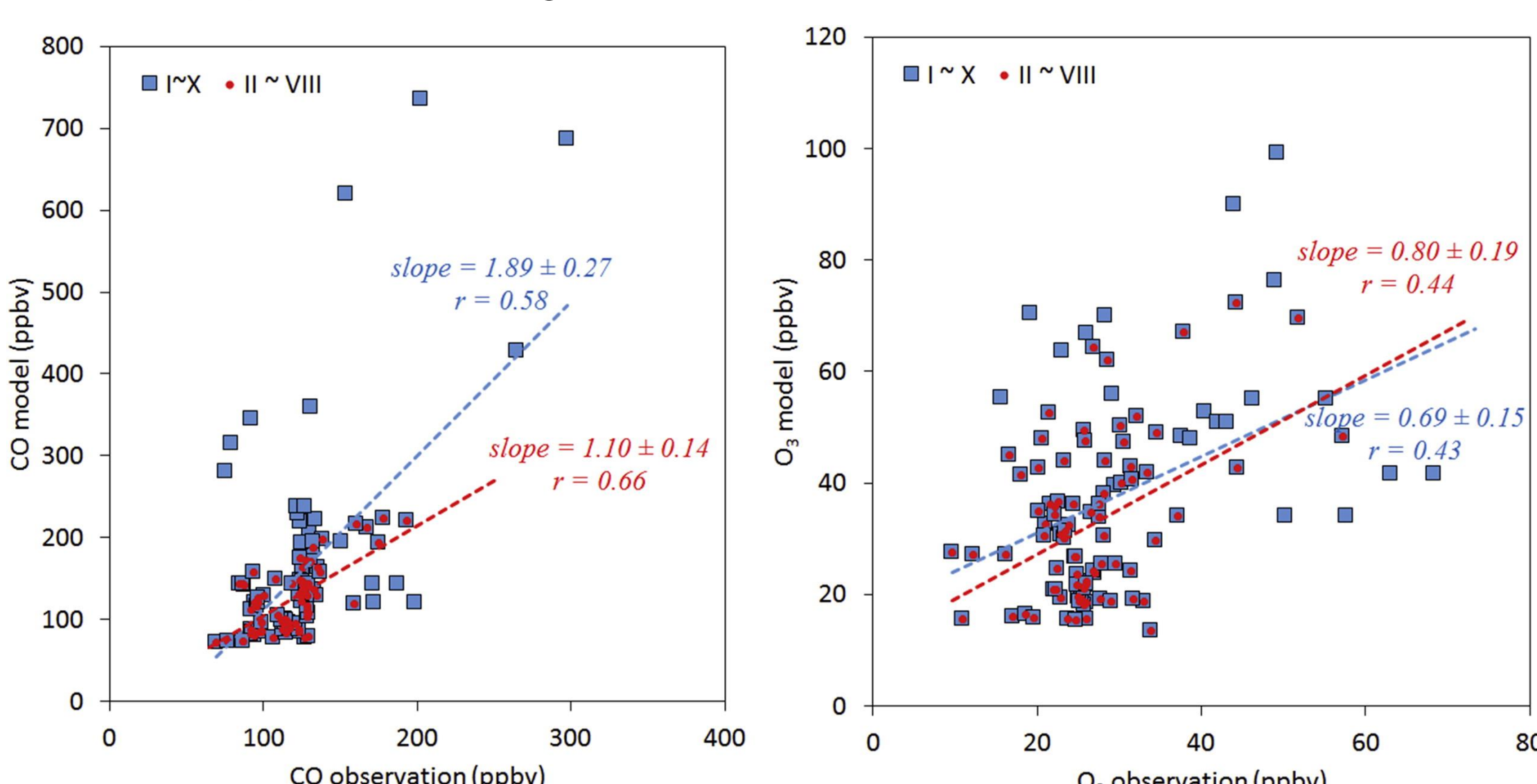
CO and O₃ Observations



CO (orange) and O₃ (blue) concentrations in the marine boundary layer along the cruise track. The upper and lower panels indicate two expeditions in July (Incheon – Nome, AK) and in September (Nome, AK – Busan), respectively. Note that the extended gaps in the July measurements result from data flagged for contamination by ship exhaust.

A 3-D global chemical transport model simulation

We used the MOZART-4 global chemical transport model to simulate the CO and O₃ concentrations along the cruise tracks. MOZART-4 contained more than 130 chemical and aerosol species and approximately 200 reactions and was driven by the Goddard Earth Observing System Model, Version 5 (GEOS-5) meteorology. In addition to the standard full chemistry model, we added tags for the sources (anthropogenic, biomass burning, biogenic, ocean, and chemical production) and for the emissions regions of CO, which allowed us to analyze the source composition and regional influence of CO.

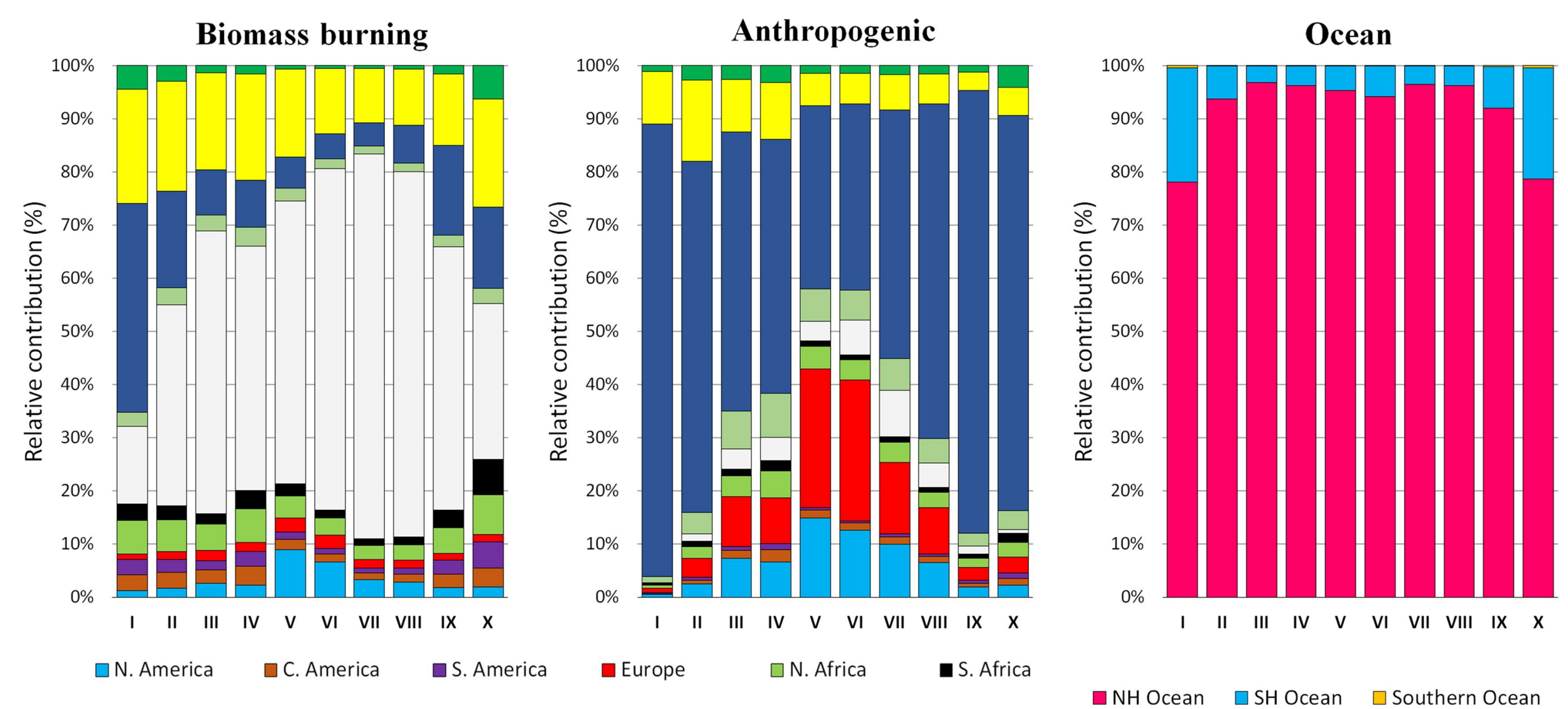


Scatter plots between the observed and modeled CO and O₃ concentrations. Blue squares represent all of the 6-h mean data and red dots exclude the data from section I, IX and X that were strongly influenced by anthropogenic emissions. For both CO and O₃, the model results correspond better to the observations when the data from section I, IX and X are excluded.

During summer, Siberian boreal forest fires are usually frequent. Thus, the anthropogenic influence becomes weaker than emissions from biomass burning in eastern Siberia. The variability of anthropogenic sources decreased as R/V Araon sailed far from the source region, and biomass burning emissions appeared to govern the variation of the total CO concentration. Especially in section VI and VII, biomass burning contributes 23% and 25% of total CO, which are close to the anthropogenic emissions of 29% and 26%, respectively.

In seawater, CO is produced by the photochemical oxidation of chromophoric dissolved organic matter. While the ocean has been known to be a minor source of tropospheric CO, the model simulation indicates that the air in the MBL of the open ocean (section III and IV in Fig. 7) contains oceanic CO up to 6–8 % of the total CO concentration. The substantial oceanic CO contribution is due to the minimum total CO concentration and strong oceanic CO production during summer. Hence, within the MBL, we argue that the role of oceanic CO should not be neglected for understanding summer season CO-related chemistry.

Long-range transport of CO



Relative contribution of CO sources from various regions to the given section of the cruise track. For biomass burning and anthropogenic sources, 11 emission regions are traced and 3 regions are defined for ocean emissions in the model.

Conclusions

- The CO-tagged MOZART4 provides useful insight about the origin and transport of CO.
- The relative importance of biomass burning CO increased in the higher latitudes.
- Over the Bering Sea, the European anthropogenic CO is comparable to the NE Asian's.
- The oceanic CO might be important to understand the MBL CO variations in summer.
- O₃ is mainly formed by photochemistry from CO in the NE Asia region.

Further reading

Keyhong Park, Tae Siek Rhee, Source characterization of carbon monoxide and ozone over the Northwestern Pacific in summer 2012, Atmospheric Environment, Volume 111, June 2015, Pages 151-160,

Acknowledgements

We acknowledge the captain and crew of the ice breaker R/V Araon for their on board assistance. This work was supported by Korea Polar Research Institute grants ([PE13410](#), [PM14040](#), and [PP14020](#)).